

DELPHI Collaboration



DELPHI 2001-054 CONF 482

5 July, 2001

---

## Search for $B_s - \overline{B}_s^0$ oscillations in inclusive samples

T. Allmendinger<sup>1</sup>, P. M. Kluit<sup>2</sup>, F. Parodi<sup>3</sup> and A. Stocchi<sup>4</sup>

<sup>1</sup> Karlsruhe, <sup>2</sup> NIKHEF Amsterdam, <sup>3</sup> INFN Genova, <sup>4</sup> LAL Orsay, CERN Geneva

### Abstract

Oscillations of  $B_d$  and  $B_s$  mesons were studied using a sample of about 3.5 million hadronic Z decays. A sample of 120 k soft leptons i.e. identified electrons and muons with a transverse momentum of less than 1.2 GeV/c and a sample of 500 k inclusively reconstructed vertices was selected.

Using both samples the mass difference of the two physical  $B_d^0$  states was measured to be:

$$\Delta m_d = 0.508 \pm 0.027(stat.) \pm 0.007(syst.)ps^{-1}$$

The following limit on the width difference of the two physical  $B_d^0$  was obtained:

$$\Delta\Gamma_{B_d}/\Gamma_{B_d} < 0.20 \text{ at } 90\% \text{ CL.}$$

No evidence for  $B_s^0 - \overline{B}_s^0$  oscillations was found and a limit on the mass difference of the two physical  $B_s$  states was put:

$$\Delta m_s > 1.1ps^{-1} \text{ at } 95\% \text{ CL}$$
$$\text{Sensitivity} = 6.1 ps^{-1}$$

Contributed Paper for EPS HEP 2001 (Budapest) and LP01 (Rome)

# 1 Introduction

In the Standard Model,  $B_q^0 - \overline{B}_q^0$  ( $q = d, s$ ) mixing is a direct consequence of second order weak interactions. Starting with a  $B_q^0$  meson produced at time  $t=0$ , the probability,  $\mathcal{P}$ , to observe a  $B_q^0$  decaying at the proper time  $t$  can be written, neglecting effects from CP violation:

$$\mathcal{P}(B_q^0 \rightarrow B_q^0) = \frac{\Gamma_q}{2} e^{-\Gamma_q t} [\cosh(\frac{\Delta\Gamma_q}{2} t) + \cos(\Delta m_q t)].$$

Here  $\Gamma_q = \frac{\Gamma_q^H + \Gamma_q^L}{2}$ ,  $\Delta\Gamma_q = \Gamma_q^H - \Gamma_q^L$ , and  $\Delta m_q = m_q^L - m_q^H$ , where  $L$  and  $H$  denote respectively the light and heavy physical states. The oscillation period gives a direct measurement of the mass difference between the two physical states. The Standard Model predicts that  $\Delta\Gamma \ll \Delta m$ . Neglecting a possible difference between the  $B_s^0$  lifetimes of the heavy and light mass eigenstates, the above expression simplifies to:

$$\mathcal{P}_{B_q^0}^{unmix.} = \mathcal{P}(B_q^0 \rightarrow B_q^0) = \frac{1}{2\tau_q} e^{-\frac{t}{\tau_q}} [1 + \cos(\Delta m_q t)] \quad (1)$$

and similarly:

$$\mathcal{P}_{B_q^0}^{mix.} = \mathcal{P}(B_q^0 \rightarrow \overline{B}_q^0) = \frac{1}{2\tau_q} e^{-\frac{t}{\tau_q}} [1 - \cos(\Delta m_q t)] \quad (2)$$

In the Standard Model,  $B_q^0 - \overline{B}_q^0$  ( $q = d, s$ ) mixing frequency  $\Delta m_{B_q}$  (having kept only the dominant top quark contribution) can be expressed as follows :

$$\Delta m_{B_q} = \frac{G_F^2}{6\pi^2} |V_{tb}|^2 |V_{tq}|^2 m_t^2 m_{B_q} f_{B_q}^2 B_{B_q} \eta_B F(\frac{m_t^2}{m_W^2}). \quad (3)$$

In this expression  $G_F$  is the Fermi coupling constant;  $F(x_t)$ , with  $x_t = \frac{m_t^2}{m_W^2}$ , results from the evaluation of the box diagram and has a smooth dependence on  $x_t$ .  $\eta_B$  is a QCD correction factor obtained at next to leading order in perturbative QCD. The dominant uncertainties in equation 3 come from the evaluation of the B meson decay constant  $f_{B_q}$  and of the ‘‘bag’’ parameter  $B_{B_q}$ . In terms of the Wolfenstein parametrization, the two elements of the  $V_{CKM}$  matrix are equal to:

$$|V_{td}| = A\lambda^3 \sqrt{(1-\rho)^2 + \eta^2} \quad ; \quad |V_{ts}| = A\lambda^2, \quad (4)$$

neglecting terms of order  $O(\lambda^4)$ .  $|V_{ts}|$  is independent on  $\rho$  and  $\eta$  and is equal to  $|V_{cb}|$ . A precise measurement of  $\Delta m_d$  can be related to  $|V_{td}|$ . It defines circle in the  $\rho$ - $\eta$  plane. Nevertheless the precision on  $\Delta m_d$  cannot be fully exploited due to the large uncertainty which originates in the evaluation of the non perturbative QCD parameters.

The ratio between the Standard Model expectations for  $\Delta m_d$  and  $\Delta m_s$  is given by the following expression:

$$\frac{\Delta m_d}{\Delta m_s} = \frac{m_{B_d} f_{B_d}^2 B_{B_d} \eta_{B_d} |V_{td}|^2}{m_{B_s} f_{B_s}^2 B_{B_s} \eta_{B_s} |V_{ts}|^2} \quad (5)$$

A measurement of the ratio  $\frac{\Delta m_d}{\Delta m_s}$  gives the same type of constraint in the  $\rho - \eta$  plane, as a measurement of  $\Delta m_d$  and this ratio is expected to be less dependent on the absolute values of  $f_B$  and  $B_B$ .

Using existing measurements which constrain  $\rho$  and  $\eta$ , except those on  $\Delta m_s$ , the distribution for the expected values of  $\Delta m_s$  can be obtained. It has been shown that  $\Delta m_s$  has to lie, at 68% C.L., between 10.9 and 18.1  $ps^{-1}$  and is expected to be smaller than 21.5  $ps^{-1}$  at 95% C.L. [1].

Using the DELPHI data, several analyses searching for  $B_s^0 - \overline{B}_s^0$  oscillations have been performed using exclusively reconstructed  $B_s$  mesons,  $D_s$ -lepton,  $D_s$ -hadron events and events with a high transverse momentum lepton [2]. In this analysis events with a high transverse momentum lepton will be removed and the remaining events will be used to search  $B_s$  and  $B_d$  oscillations. A similar inclusive analysis based on the 1994-1995 data using neural networks was submitted to the ICHEP 2000 conference [3].

## 2 Analysis

For a description of the DELPHI detector and its performance the reader is referred to [4]. The analysis described in this paper uses the precise tracking based on the silicon microvertex detector to reconstruct the primary and secondary vertex. To estimate the B momentum and direction, the tracks and the neutral particles detected in the electromagnetic and hadronic calorimeter were used. Muon identification was based on the hits associated to a track in the muon chambers. Electrons were identified using tracks associated to a showers in the electromagnetic calorimeter. The  $dE/dx$  energy loss measurement in the time projection chamber and the Cherenkov light detected in the RICH were used to separate pions (electrons or muons) from kaons and protons.

Tracks were selected if they satisfied the following criteria: their momentum lies above 200 MeV/c, tracklength was at least 30 cm, relative momentum error was less than 130%, their polar angle was between  $20^\circ$  and  $160^\circ$  and their impact parameter w.r.t to the primary vertex was less than 4 cm in the xy plane (perpendicular to the beam) and 10 cm in z (along the beam direction). Neutral particles had to deposit at least 500 MeV in the calorimeters and their polar angle had lie between  $2^\circ$  and  $178^\circ$ .

To select hadronic events it was required that more than 7 tracks were accepted with a total energy from the tracks above 15 GeV. The event was divided into two hemispheres using the thrust axis. Per hemisphere the total energy from tracks and neutral particles had to be larger than 5 GeV. The thrust direction was determined and the polar angle of the thrust axis was required to satisfy  $|\cos(\theta_{thrust})| < 0.8$ .

Using tracks with vertex detector information, the primary vertex was fitted using the average beamspot per fill as a constraint. For each track the impact parameter w.r.t. the primary vertex was calculated and the lifetime sign determined. The b tagging probability  $P_E^+$  (E refers to the fact that the total event is used, + that the lifetime sign had to be positive) was defined as the probability that all the selected tracks were coming from the primary vertex. In the 1992 and 1993 data the vertex detector measured only the  $R\phi$  coordinate, while in 1994 and 1995 also the  $Rz$  coordinate was measured. In the 1992-1993 data events were selected if the b tagging variable  $P_E^+$  was less than 0.1. In the 1994-1995 data the cut could be placed at 0.015.

Jets were reconstructed using tracks and neutral particles with the LUCCLUS jet algorithm with an invariant mass cut DJOIN of 6 GeV/c<sup>2</sup>. Identified leptons were assigned to the closest jet and their transverse momentum w.r.t. the jet axis was determined. Loosely, standard and tightly identified muons with a momentum above 2 GeV/c were

accepted. For the identification criteria for loose, standard and tight muons the reader is referred to [4]. Loosely identified muons with a momentum below 3 GeV/c were rejected. Standard and tightly identified muons with a momentum above 3 GeV/c and a transverse momentum above 1.2 GeV/c were removed from the sample. This was done to avoid overlap with other analyses that use leptons [2]. For electron identification a neural network was used with a cut value that corresponds to 75% efficiency [4]. The electron had to have a momentum above 2 GeV/c. Electrons with a momentum below 3 GeV/c had to pass a cut value that corresponds to 65% efficiency. To avoid overlap, electrons with momenta above 3 GeV/c and transverse momenta above 1.2 GeV/c satisfying a cut value that corresponds to 65% efficiency were removed. These identified electrons and muons will be called further on soft leptons.

Samples of  $Z \rightarrow q\bar{q}$  and  $Z \rightarrow b\bar{b}$  were simulated using the Monte Carlo generator programme JETSET7.3 with DELPHI tuned JETSET parameters and updated b and c decay tables [6]. The response of the DELPHI detector was simulated in detail [7]. In total about 4 million simulated hadronic Z decays were used for this analysis.

## 2.1 Secondary vertex reconstruction

The secondary vertex and proper time determination is the identical for events with or without a soft lepton. First the probability  $P_i$  that a track or neutral particle comes from the secondary (bottom or charm) vertex was parametrized. The following information was used for tracks, the lifetime signed impact parameter and its error (in  $R\phi$  and  $Rz$ ), the transverse momentum w.r.t. jet, muon and electron identification and rapidity w.r.t. jet. For neutral particles the transverse momentum and rapidity were used. For each of these quantities the probability was parametrized using the simulation. The total probability was obtained by combining these individual probabilities assuming they are independent.

To start the first level vertex fit tracks were selected with at least one associated hit in the vertex detector and a probability  $P_i$  larger then 60%. The first level vertex fit had as an input the decay length per track and its error. This decay length was determined by calculating the crossing point in space of the track with the B particle. The B particle was approximated by a track through the primary vertex in the direction of the reconstructed B jet. The secondary vertex was fitted using the the decay length and its error per track and the azimuthal and polar angles. The result of this approximate fit was a decay length, its error and a  $\chi^2$  of the fit. Further, the  $\chi_t^2$  contribution of a track was determined. To remove tracks from the primary vertex the following iterative procedure was performed. If the vertex has more than two tracks, the track behind the vertex - e.g. closest to the fitted primary vertex - and with the largest  $\chi_t^2$  contribution was removed if the  $\chi_t^2$  was larger than 4. Secondly, tracks were removed that did not combine with any of the other tracks. To achieve this, all two track combinations were made and the number of good matches was counted. A good match was defined as a two track vertex that lies within 2 standard deviations of the fitted secondary vertex. For each track the fraction  $f_{good}$  of good matches to the total number of combinations was determined. The track with the smallest  $f_{good}$  value was removed if its value lies below 20% and the first level vertex fit was redone.

At the end of this procedure a full vertex fit was performed using the full track information with the full covariance matrix. To the list of tracks selected for the fit, the B-track with its covariance matrix was added as a constraint. As a result the decay length

and its error were obtained. For each track the impact parameter and its error w.r.t. to the fitted secondary vertex was calculated. The  $\chi^2$  of the fit was defined as the quadratic sum of the impact parameter over its error (in  $R\phi$  and  $Rz$ ).

The presence of charm particles in the track fit has two effects. Firstly, the fitted vertex does not coincide with the B vertex, but is a kind of average of the B and C vertex. Secondly, the  $\chi^2$  of the vertex increases due to the charm decay length. It is therefore important to remove charmed particles from the vertex fit. For this purpose the probability that a track came from charm is evaluated on the basis of kinematic and vertex information. The momentum distribution of the particle from charm in the B rest frame is e.g. softer than that for particles from B decays. Secondly, a particle from charm will decay in front of the common vertex, while a particle from a B hadron will decay behind the common vertex. Two new vertex fits were performed. In the first fit, one particle that comes most likely from charm was removed. In the second fit, the two particles coming most likely from charm were removed.

Using the simulation an estimate was made of the B decay length and its error, using as an input the fitted decay length, its associated (or raw) error and the  $\chi^2$ . This was done for the three vertex fits (removing 0, 1 and 2 particles). Removing 1 or 2 particles has the advantage of reducing the bias caused by the presence of particles from charm. On the other hand the resolution is increased if a track is removed. Due to the fact that the  $\chi^2$  is sensitive to the presence of particles from charm, part of the bias is corrected for in the parametrization of the B decay length. Finally, the result with the smallest expected error on the B decay length was chosen. In 51% of the cases no track was removed, in 36% one track and in 13% two tracks were removed.

In Figures 1a and b the expected or raw error as it comes out of the full vertex fit and the reconstructed minus the simulated B decay distance divided by the raw error are shown for the 1994-1995 data. The tail due to the presence of charmed particles can be clearly observed. Figures 1c and d show the expected error and the reconstructed minus the simulated B decay distance after applying the correction procedure described above. The distribution is clearly more gaussian and the width of the distribution is adjusted to be 1.

## 2.2 Proper time reconstruction

To determine the proper time, the momentum of the B hadron had to be measured. First, an estimate of the energy of the b jet was made using energy and momentum conservation. For the jet containing the B hadron the mass  $M_1$  was measured. The invariant mass of all the other tracks and neutral particles in the event  $M_2$  was measured. The b jet energy was obtained by:

$$E_{jet} = E_{cms}/2 - (M_2^2 - M_1^2)/(2 E_{cms}), \quad (6)$$

where  $E_{cms}$  is the centre of mass energy. The B energy was determined as:

$$E_B = \frac{\sum_i P_i E_i}{\sum_i E_i} E_{jet}, \quad (7)$$

where  $E_i$  is the energy of the tracks and neutral particles and  $P_i$  is the probability that a particle comes from the decay of a B hadron (see section 2.1).

The momentum of the B hadron was determined from the B energy and corrected as a function of the following quantities: the weighted number of tracks and neutrals, the ratio

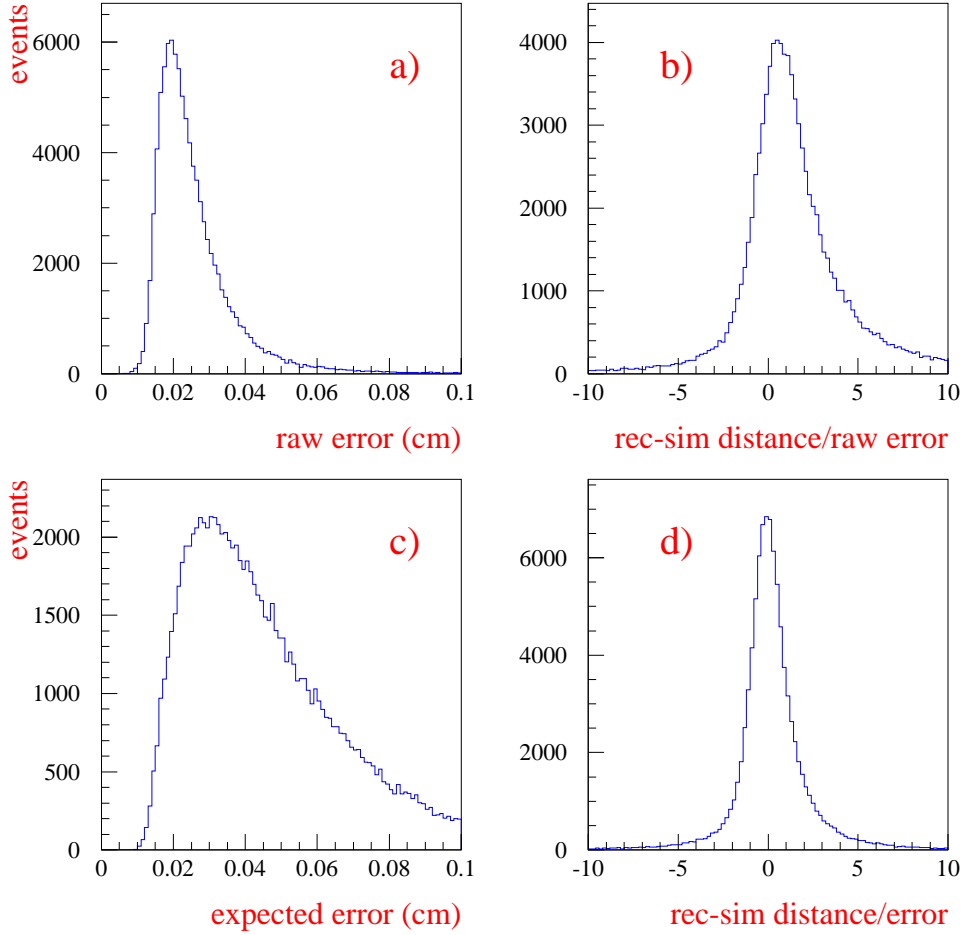


Figure 1: Figure a) shows the expected or raw error, Figure b) the reconstructed minus the simulated B decay distance divided by the raw error for the 1994-1995 simulation. Figures c) and d) show the expected error and the reconstructed minus the simulated B decay distance after applying the procedure described in the text.

of the raw B energy ( $\sum_i P_i E_i$ ) to the jet energy  $E_{jet}$ , the invariant mass  $M_1$ , the ratio of the charged over the total raw B energy and the number of jets. The reconstructed B momentum is shown in Figure 2.

The expected error was parametrized as a function of the raw B energy and energy of the jet. It lies between 3 and 9 GeV and is on the average 5 GeV/c. The reconstructed - simulated B momentum divided by the expected error from the simulation is shown in Figure 2.

The proper time  $t$  was calculated using:

$$t = \frac{mL}{p}, \quad (8)$$

where  $m$  is the B mass and  $L$  the decay length and  $p$  the estimated B momentum. The

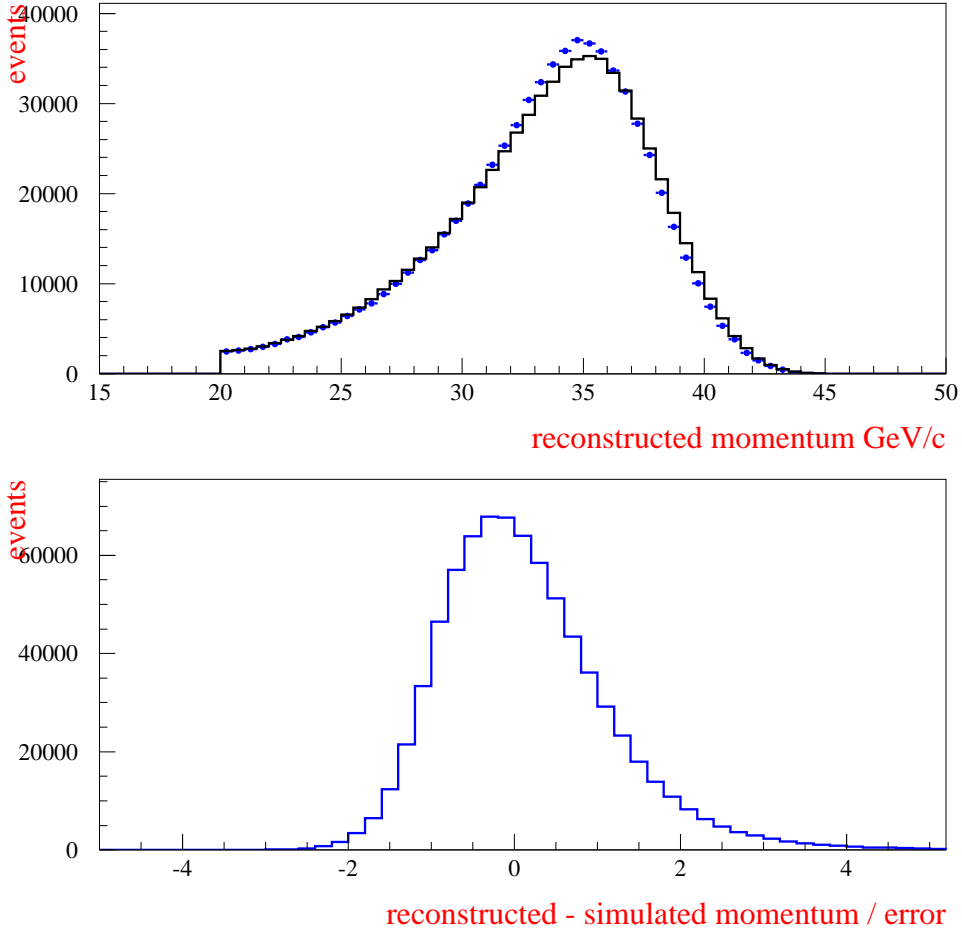


Figure 2: Reconstructed B momentum. The dots corresponds to the 1992 to 1995 data, the solid line to the simulation. The reconstructed - simulated B momentum divided by the expected error from the simulation.

expected error on the proper time was estimated using:

$$\sigma_t = \sqrt{\left(\frac{m\delta L}{p}\right)^2 + \left(\frac{mL\delta p}{p^2}\right)^2}, \quad (9)$$

where  $\delta L$  is the estimated error on the decay length and  $\delta p$  the error on the momentum. The data was divided into eight categories according to the proper time resolution. The cuts are shown in Table 1. To fall into category 1 the expected resolution had to be smaller than  $0.12+0.07 t$  ps ( $t$  in units of ps). Events with a resolution worse than  $0.35+0.2 t$  ps were rejected.

The first four categories contain the soft leptons and the last four the inclusive vertices. In total 126171 events containing a soft lepton and 500971 events with an inclusive vertex were selected. The proper time resolution for the eight classes are shown in Figures 3 and 4.

category	1	2	3	4
$\sigma_t(ps)$	$0.12+0.07 t$	$0.18+0.08 t$	$0.25+0.1 t$	$0.35+0.2 t$
events	18831 (5533)	33729 (10598)	34605 (12091)	39006 (15620)
category	5	6	7	8
$\sigma_t(ps)$	$0.12+0.07 t$	$0.18+0.08 t$	$0.25+0.1 t$	$0.35+0.2 t$
events	56653 (16468)	118532 (36633)	139176 (47702)	186610 (73809)

Table 1: The cuts on the resolution  $\sigma_t$  and total number of selected events (in brackets the events for the 92-93 data) for the different categories.

### Soft leptons

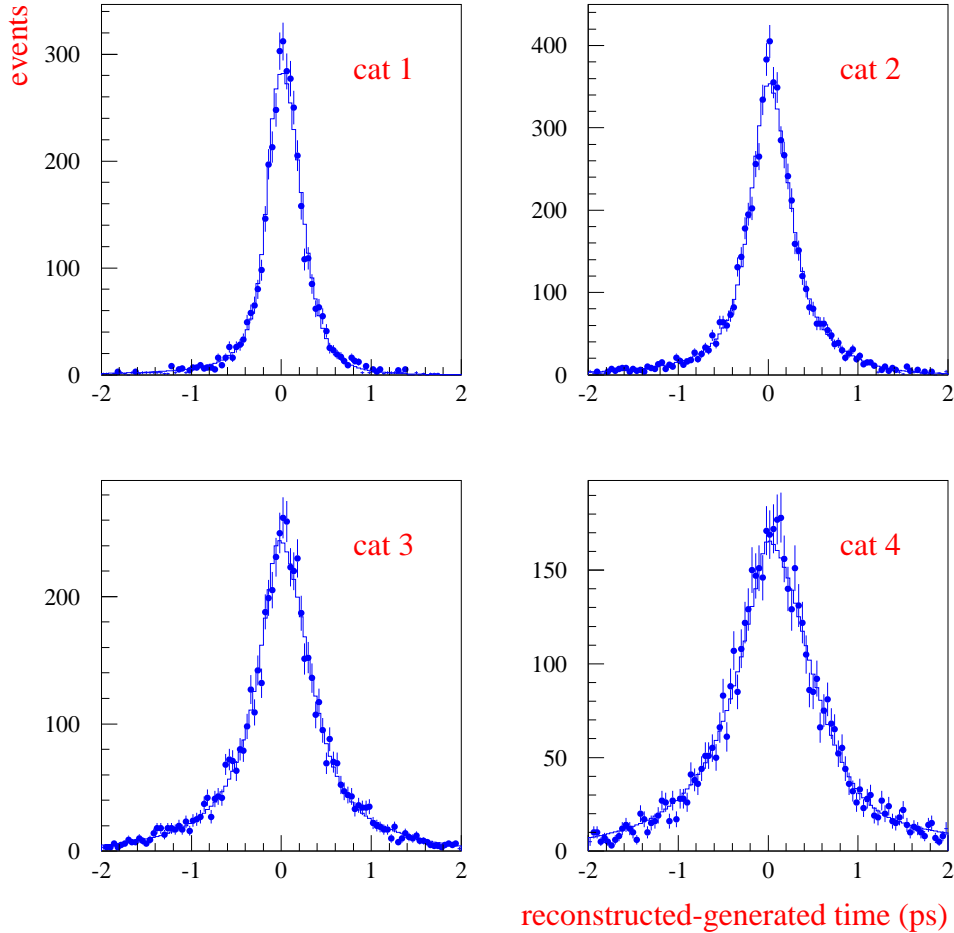


Figure 3: Reconstructed-generated proper time for the soft leptons: categories 1 to 4. The dots correspond to the data, the solid line to the parametrization (see section 2.5).



## Inclusive vertices

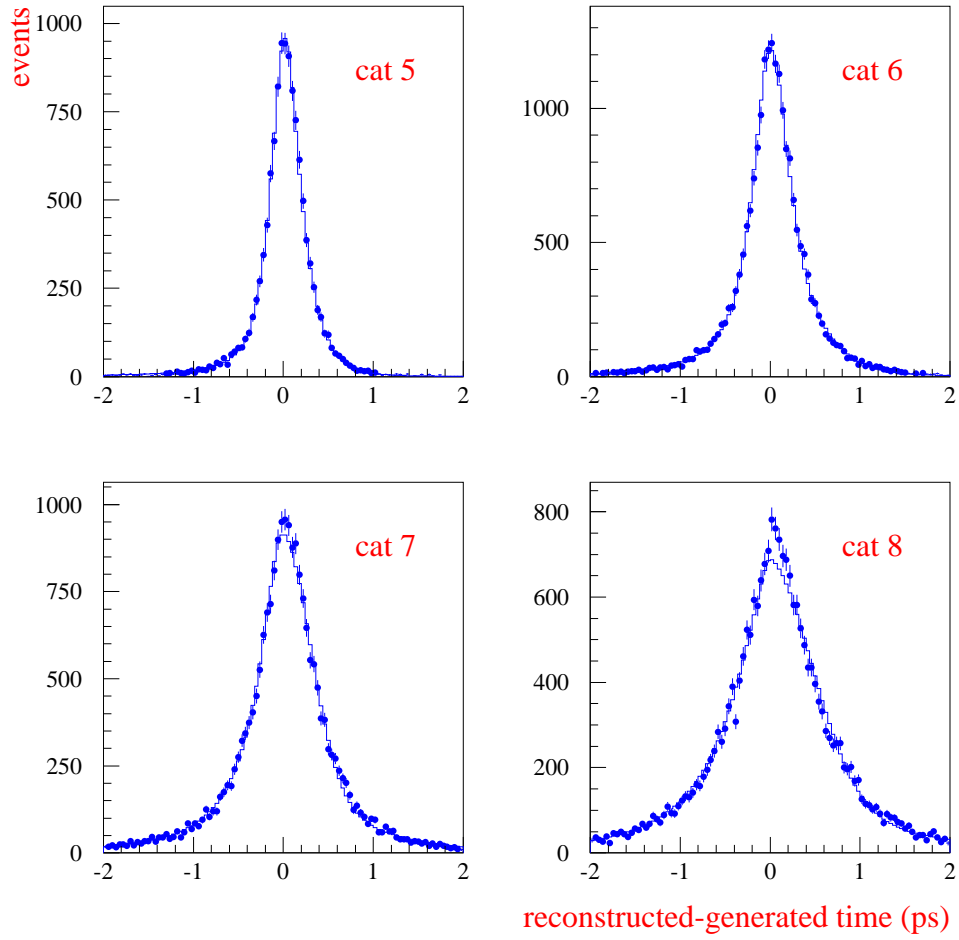


Figure 4: Reconstructed-generated proper time for the inclusive vertices: categories 5 to 8. The dots correspond to the data, the solid line to the parametrization (see section 2.5).

## 2.3 Production and decay tag

To separate oscillating from non-oscillating  $B_s$  mesons, a production and a decay tag were developed. The production tag gives the flavor of the B ( $b$  or  $\bar{b}$ ) at the time of production. The decay tag gives the flavor of the B at the decay time (so after it has oscillated). In this analysis both the production and decay tag were optimized for  $B_s$  mesons. In  $Z$  decays a  $b$  and  $\bar{b}$  quark are produced back to back in pairs. Therefore the hemisphere opposite to the hemisphere of the decaying B can be used to tag the flavor at the production time. This will be called the opposite side production tag. The same side production tag used the fragmentation tracks accompanying the decaying  $B_s$  meson.

For the production tag a combination of several variables was used:

- The jet charge using tracks from the decaying B is defined as:

$Q_{jet} = \sum q_i p_{i//} / \sum p_{i//}$  with  $P_i > 0.5$ , where  $p_{i//}$  is the momentum of the particle along the direction of the jet axis.

- The jet charge for fragmentation tracks defined as:

$Q_f = \sum q_i p_{i//} (P_i < 0.5) / \sum p_{i//} (P_i > 0)$ .

- The momentum  $p^*$  of the identified lepton in the B rest frame.
- The heavy particle charge obtained for identified kaons or protons as a function of the momentum in the B rest frame  $p^*$ .

These variables were converted into probabilities and then combined to give the opposite side production tag. In Figure 5 the opposite side production tag is shown for 1992-1995 data and simulation. The tagging purity is defined as the fraction of correct charge assignments at 100% efficiency. It is 68% for the 1992-1995 simulation. If in the algorithm only the opposite hemisphere jet charge was used the purity would be 64% [2].

The same side production tag uses the fragmentation tracks accompanying the decaying  $B_s$ . Both leading fragmentation pions and kaons are sensitive to the B production flavor. The following quantity  $Q_{same}$  was defined:

$Q_{same} = \sum R(p_{i//}, ih)(1 - P_i)q_i$ , where  $ih$  is 1 for a heavy (proton, kaon) or 0 for a light (electron, muon pion) particle. The parametrization for  $R$  was obtained from the simulation. The variable  $Q_{same}$  was converted into a probability and then combined with the opposite side production tag.

In Figure 5 the combined production tag is shown for 1992-1995 data and simulation. The tagging purity for a  $B_s$  is 71% for the 1992-1995 simulation. This is - as expected - better than the result for the opposite side production tag. The difference between data and simulation will be taken into account by fitting the purity on the data (see section 2.6).

The other essential ingredient in the analysis is the decay tag. For the soft leptons this tag is relatively straight forward. Most of the  $B - \bar{B}$  separation comes from the momentum of the lepton in the B rest frame  $p^*$  that allows us to separate between a prompt lepton coming from the B vertex and a lepton coming from a charm decay. It is clear that other information in the event as e.g. the impact parameter of the lepton with respect to the secondary vertex and the isolation of the lepton (presence of tracks from charm decay) helps to improve the  $B - \bar{B}$  separation. Finally, also the inclusive vertex decay tag (discussed below) was added to improve slightly the performance.

For the inclusive vertices the development of a decay tag is more difficult. The following approach was taken. All the tracks and neutrals particles were boosted back in the B reference frame. The thrust axis was determined and the tracks were assigned to the

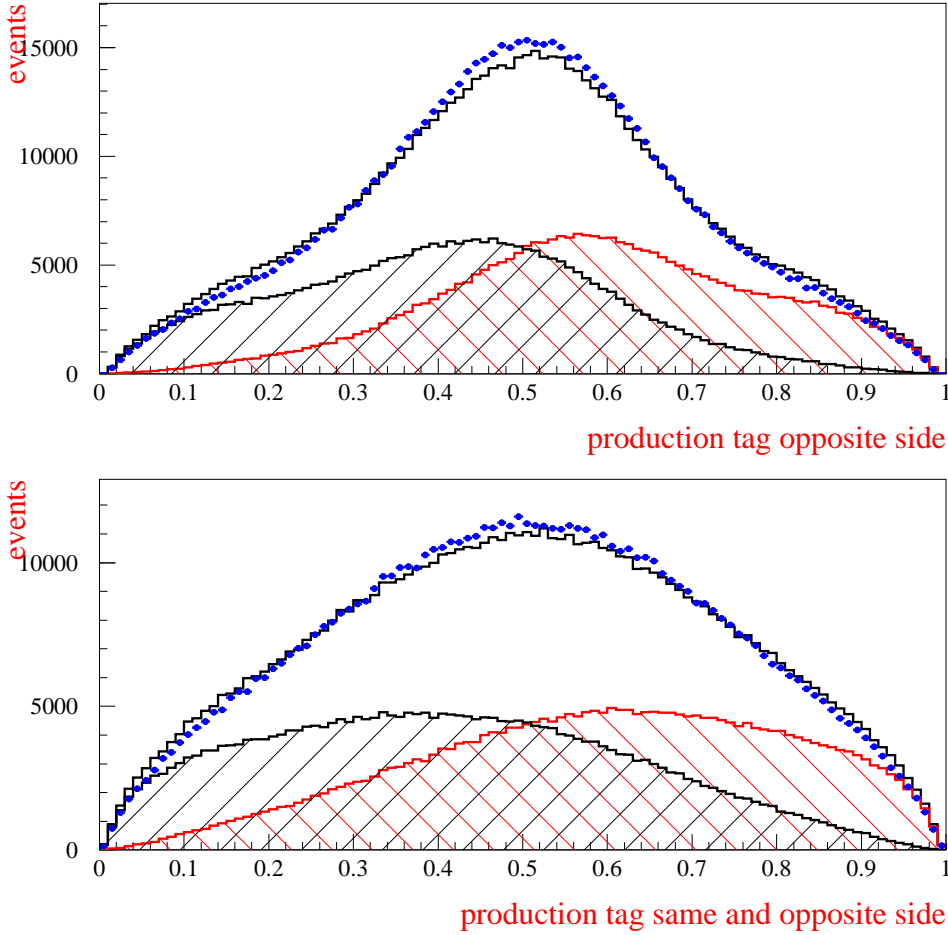


Figure 5: Production tag using only information from the opposite side and the production tag using information from both sides. The dots correspond to the 1992 to 1995 data, the solid line to the simulation. The hatched areas correspond to the  $b$  and  $\bar{b}$  contributions.

forward of backward hemisphere. In most of the cases the forward hemisphere contains most of the tracks from the B vertex while the other hemisphere contains most of the tracks from charm decay (or vice versa). This is called a dipole, because the  $B_s^0$  decays in a  $D_s^{-(*)}$  and a virtual  $W^+$  and the charge difference between the two hemispheres is  $\pm 2$ . Under the hypothesis that the forward (backward) hemisphere contains the particles from the charm decay and the backward (forward) hemisphere the particles from the B vertex, the flavor probability of the decaying  $B_s$  is evaluated. This is done using the charge and the momentum  $p^*$  in the B rest frame of the heavy and light particles. For the parametrizations the simulation was used. Then a hemisphere probability is evaluated for the hypothesis that the charmed particle is in the forward (backward) hemisphere. This probability is a function of the impact parameter of the tracks w.r.t the secondary vertex, the momenta in the B rest frame and the hemisphere multiplicity. By combining the hemisphere probability with the flavor probability, the decay tag for the inclusive vertices was obtained.

In Figure 6 the performance of the decay tag for soft leptons is shown for 1992-1995 data and simulation. The tagging purity is 69% at 100% efficiency. In Figure 6 the performance of the decay tag for inclusive vertices is shown for 1992-1995 data and simulation. The  $B_s$  tagging purity is 58% at 100% efficiency. The difference between data and simulation will be taken into account by fitting the purity on the data as will be discussed in section 2.6.

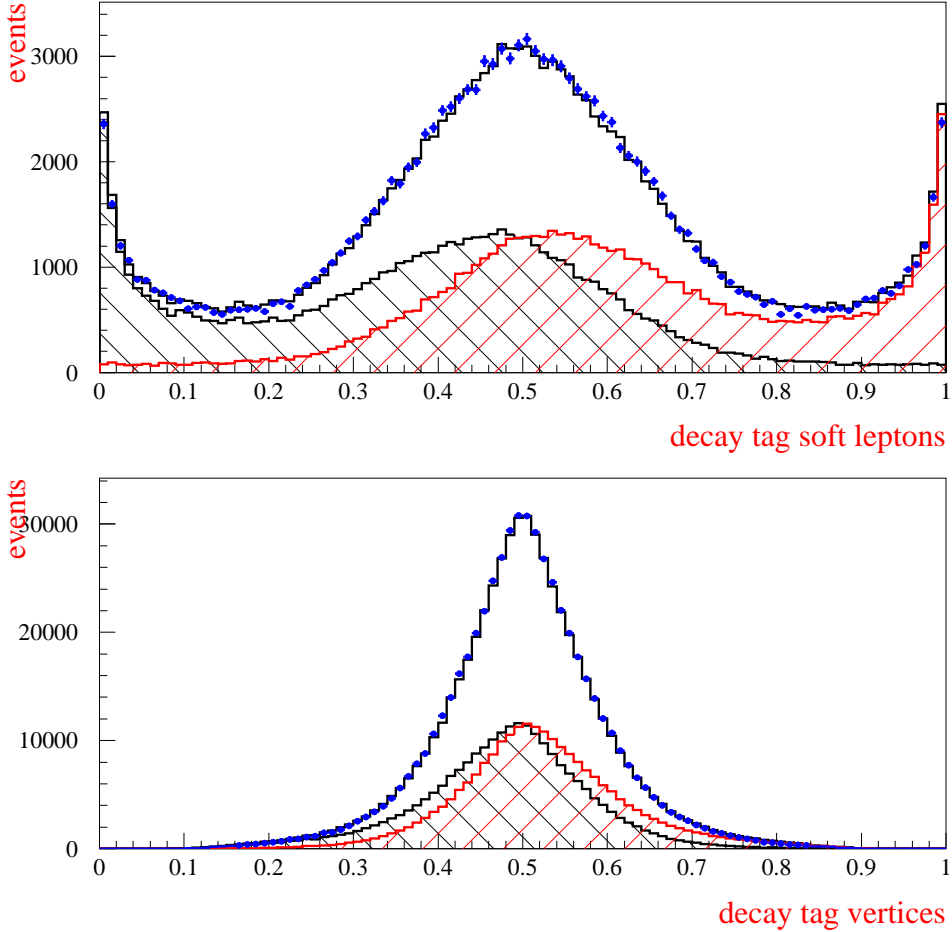


Figure 6: Decay tag for the soft leptons and vertices. The dots correspond to the 1992 to 1995 data, the solid line to the simulation. The hatched areas correspond to the  $b$  and  $\bar{b}$  contributions at the time of decay.

## 2.4 Sample composition

For the sample composition of the B hadrons the following fractions were assumed [8]:  $f_{B_s^0} = 0.097$ ,  $f_{B \text{ baryons}} = 0.103$ ,  $f_{B^+} = 0.40$  and  $f_{B_d^0} = 0.40$ .

For the lifetime of the different B species it was assumed that [8]:  $\tau_{B^+} = 1.65$  ps,  $\tau_{B_d^0} = \tau_{B_s^0} = 1.55$  ps and  $\tau_{B \text{ baryons}} = 1.20$  ps.

Using the simulation the uds and charm backgrounds were extracted. The background fractions for the different data sets and vertex categories are listed in Table 2.

background	data set	cat 1	cat 2	cat 3	cat 4	cat 5	cat 6	cat 7	cat 8
$f_{uds}$	1992-1993	.0074	.0158	.0288	.0495	.0226	.0407	.0717	.1237
$f_{uds}$	1994-1995	.0046	.0076	.0117	.0229	.0138	.0199	.0329	.0588
$f_{charm}$	1992-1993	.0202	.0653	.1116	.1779	.0359	.0920	.1433	.1900
$f_{charm}$	1994-1995	.0356	.0673	.1201	.1919	.0436	.0928	.1514	.2004

Table 2: The background fractions for the 1992-1995 data sets splitted up for the different vertex categories.

## 2.5 Fitting programme

In the fitting program the resolution function  $\mathcal{R}(t_{rec} - t_{true}, t_{true})$  was parametrized. The resolution function gives the probability that given a certain value for the true proper time  $t_{true}$  a proper time value  $t_{rec}$  is reconstructed. Two asymmetric gaussians are used to describe the main signal, one asymmetric gaussian to describe the broad background and one gaussian to describe the probability that one reconstructs the secondary vertex near the primary vertex. The width of the gaussians are of the form  $\sigma = \sqrt{\sigma_0^2 + \sigma_p^2 t_{true}^2}$ . The term with  $\sigma_p$  takes into account the finite momentum resolution. The relative normalizations of the gaussians are free and parametrized as a constant plus a term proportional to  $1 - e^{-t_{true}/\tau}$ , where  $\tau$  is the average b lifetime. For each vertex category the resolution function was fitted. The result of the fit is shown in Figures 3 and 4.

The probability for a B event to be observed at a proper time  $P(t_{rec})$  was written as a convolution over an exponential B decay distribution, an acceptance function  $A(t_{true})$  and the resolution function:

$$\mathcal{P}_b(t_{rec}) = \int_{t=0}^{\infty} A(t) \mathcal{R}(t_{rec} - t, t) \frac{e^{-t/\tau}}{\tau} dt \quad (10)$$

The acceptance function was parametrized for the different vertex categories using the simulation. Due to the requirements on the flight distance in the track selection, the acceptance is a smooth - but not flat - function of the proper time. The probabilities for uds  $\mathcal{P}_l$  and charm  $\mathcal{P}_c$  events for the different vertex categories are parametrized as a function of  $t_{rec}$  with exponential functions using the simulation.

In the fitting program the like- and unlike-sign events were fitted, using as an input the reconstructed proper time and the combined tagging probability. The combined tagging probability is defined as

$$P_{comb} = P_{prod} P_{decay} + (1 - P_{prod})(1 - P_{decay}) \quad (11)$$

The like-sign events are those events for which  $P_{comb}$  is larger than 50%, unlike-sign events are those for which  $P_{comb}$  is less than 50%.

The total probability for a like-sign events is:

$$\mathcal{P}^{like}(t_{rec}) = f_b \sum_q \epsilon_{Bq} \mathcal{P}_{B_q}^{mix.}(t_{rec}) + f_b \sum_q (1 - \epsilon_{Bq}) \mathcal{P}_{B_q}^{unmix.}(t_{rec}) + f_c (1 - \epsilon_c) \mathcal{P}_c(t_{rec}) + f_l (1 - \epsilon_l) \mathcal{P}_l(t_{rec}) \quad (12)$$

and correspondingly for the unlike-sign event:

$$\mathcal{P}^{unlike}(t_{rec}) = f_b \sum_q (1 - \epsilon_{Bq}) \mathcal{P}_{B_q}^{mix.}(t_{rec}) + f_b \sum_q \epsilon_{Bq} \mathcal{P}_{B_q}^{unmix.}(t_{rec}) + f_c \epsilon_c \mathcal{P}_c(t_{rec}) + f_l \epsilon_l \mathcal{P}_l(t_{rec}) \quad (13)$$

The tagging purity  $\epsilon_{Bq}$  was expressed in the combined tagging probability. For  $B_s$  tagging purity one has:

$$\epsilon_{B_s} = 0.5 + |P_{comb} - 0.5| \quad (14)$$

The tagging purity for the other B particles and the charm and light quark background was also expressed as a function of  $P_{comb}$  ( $P_{prod}$  and  $P_{decay}$ ) using the simulation (see section 2.6).

For the mixed  $B_d$  and  $B_s$  mesons one has the following expression:

$$\mathcal{P}_{B_q}^{mix.}(t_{rec}) = \int_{t=0}^{\infty} A(t) \mathcal{R}(t_{rec} - t, t) \mathcal{P}_{B_q}^{mix.}(t), \quad (15)$$

while for the unmixed case also the  $B_u$  and B baryons were included:

$$\mathcal{P}_{B_q}^{unmix.}(t_{rec}) = \int_{t=0}^{\infty} A(t) \mathcal{R}(t_{rec} - t, t) \mathcal{P}_{B_q}^{unmix.}(t). \quad (16)$$

where  $\mathcal{P}_{B_q}^{(un)mix.}(t)$  is defined in Eqs. 1 and 2.

## 2.6 Modelling the simulation and data

In the analysis an event-by-event tagging purity is used  $\epsilon_{B_s}$  as defined in Eq. 14. In general, the tagging purities for the the different B species, charm and light quarks are different. To obtain a correct fit to the simulated or real data using Eqs. 12 and 13, it is important to model precisely the tagging purities.

For leptons the decay purity for the different B species is identical. For the production tag the purity has to be calculated. This is most easily done by modifying the probability  $P$  ( $P_{prod}$  or  $P_{decay}$ ). For this purpose a slope  $\alpha$  is introduced and the new probability is defined as:

$$P_{new} = (P/(1 - P))^\alpha / (1 + (P/(1 - P))^\alpha) \quad (17)$$

A slope of 1 means that the probability remains unchanged. The decay tag slope for the soft leptons was 1. The decay tag slopes for the inclusive vertices and soft leptons as well as the production tag slope are listed in Table 3. The values are obtained from the simulation. For the charm quark a slope  $\alpha_D$  of 4.1 is used if the probability lies between 0.2 and 0.8, else  $\alpha_D=1$ . Note that the slopes  $\alpha_D$  and  $\alpha_P$  for the different B species are quite similar, expect for the  $B_u$ . From the new probability  $P_{new}^{B_q,uds,c}$ , the combined probability  $P_{comb}^{B_q,uds,c}$  is calculated using Eq. 11 and the purity  $\epsilon_{B_q,uds,c}$  is obtained using:

$$\epsilon_{B_q,uds,c} = 0.5 + |P_{comb}^{B_q,uds,c} - 0.5|. \quad (18)$$

Particle	inclusive vertex decay tag slope $\alpha_D$	soft lepton $\alpha_D$	production tag slope $\alpha_P$
$B_s$	1	1	1
$B_d$	1.15	1	1.13
$B_u$	0.75 to 1	1	0.3 to 0.8
$B$ baryon	0.80	1	1.09
$uds$	0.20	0.20	0.80
$charm$	4.2 (P=0.2-0.8)	4.2 (P=0.2-0.8)	0.50

Table 3: The slopes for the production and decay tag for the different particles as obtained from simulation.

It is important to have a correct modeling of the tagging purity of the data i.e. to have a good description of the like- and unlike-sign events. Using the data, it is possible to fit for each category a correction factor  $C$  to the slope:

$$\alpha_D^{data} = C \alpha_D, \quad (19)$$

where  $C$  is determined from the fraction of like-sign events. For the soft leptons the results are shown in Table 4.

data set	category	fitted value for $C$
1992-93	1	$0.95 \pm 0.053$
	2	$0.81 \pm 0.046$
	3	$0.76 \pm 0.047$
	4	$0.82 \pm 0.049$
1994-95	1	$0.77 \pm 0.041$
	2	$0.69 \pm 0.039$
	3	$0.83 \pm 0.042$
	4	$0.84 \pm 0.052$

Table 4: The fitted correction factor  $C$  for the soft leptons.

The total error on the  $C$  for all the soft leptons is better than 5%.

The decay tag for the  $B_u$  inclusive vertices is very different from the tag for the other B particles (see Table 3). By separating the inclusive vertex sample in one enriched in  $B_u$  particles and one depleted in  $B_u$  particles it was possible to determine on the data the correction factor  $C$  for the  $B_u$  and the other particles. Three fits were done, first it was assumed that the correction factors  $C$  for the B particles are identical. Then it was assumed that  $C$  for the non  $B_u$  particles is 1 and the correction factor  $C$  for the  $B_u$  is fitted. From the  $\chi^2$  of the fit it was clear that the second fit result was preferred. To be conservative, the correction factor  $C$  for non- $B_u$  particles is not fixed to 1 but to the average of the first fit result and 1 and then the final fit was done. The results are shown in Table 5, the error in the third row corresponds to the statistical error obtained in the first fit. The systematical error on the  $B_s$ ,  $B_d$  and  $B_{baryon}$  correction factor  $C$ , induced by the fitting procedure is larger than the statistical error and amounts to 15%. This number is obtained by comparing the results of the two fits with the final fit result.

data set	category	correction factor $C$ for $B_d$ , $B_s$ and $B_{baryon}$	$C$ for the $B_u$
1992-1993	5	$0.75 \pm 0.07$	0.54
	6	$0.76 \pm 0.06$	0.54
	7	$0.72 \pm 0.07$	0.40
	8	$0.63 \pm 0.09$	0.20
1994-1995	5	$0.93 \pm 0.05$	0.60
	6	$0.94 \pm 0.04$	0.60
	7	$0.83 \pm 0.07$	0.40
	8	$0.63 \pm 0.09$	0.20

Table 5: The fitted correction factors  $C$  for the inclusive vertices.

It was found out using the simulation that the acceptance of the  $uds$  and  $charm$  quarks is a function of the tagging purity. The acceptance  $A(t_{rec})$  for B events varies a bit as a function of the tagging purity. This was taken into account in the like- and unlike-sign probability distribution. The acceptance function was also corrected to obtain a better agreement between the data and the fitting program. Note that for  $B_d$  and  $B_s$  oscillations the fraction of like-sign events is relevant and the acceptance correction drops out in first order.

In Figures 7 and 8 the like- and unlike-sign events as a function of the proper time for the soft leptons and inclusive vertices are shown for the 1992 to 1995 data. In the plots the events have obtained a weight of  $|\epsilon_{Bs} - 0.5|$ . In this way events with a higher tagging purity get a higher weight. A good description of the data is obtained.

In Figures 9 and 10 the fraction of like-sign events as a function of the proper time for the soft leptons and inclusive vertices is shown for the 1992 to 1995 data. In these Figures a value of  $\Delta m_d$  of  $0.495 \text{ ps}^{-1}$  and  $\Delta m_s$  of  $15 \text{ ps}^{-1}$  is used.



## 92-93 data

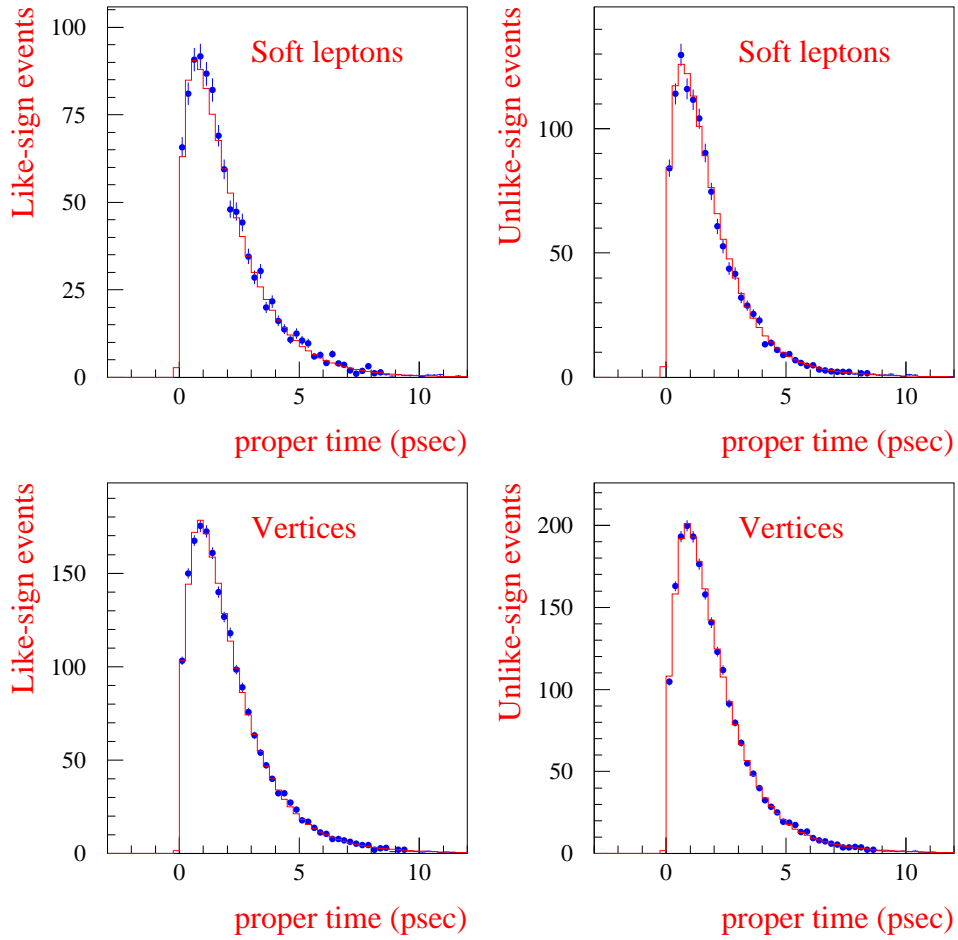


Figure 7: Like and unlike-sign events as a function of the proper time for the soft leptons and inclusive vertices. The 1992 and 1993 data are shown in dots, the fitted parametrization is shown as a solid line.

## 94-95 data

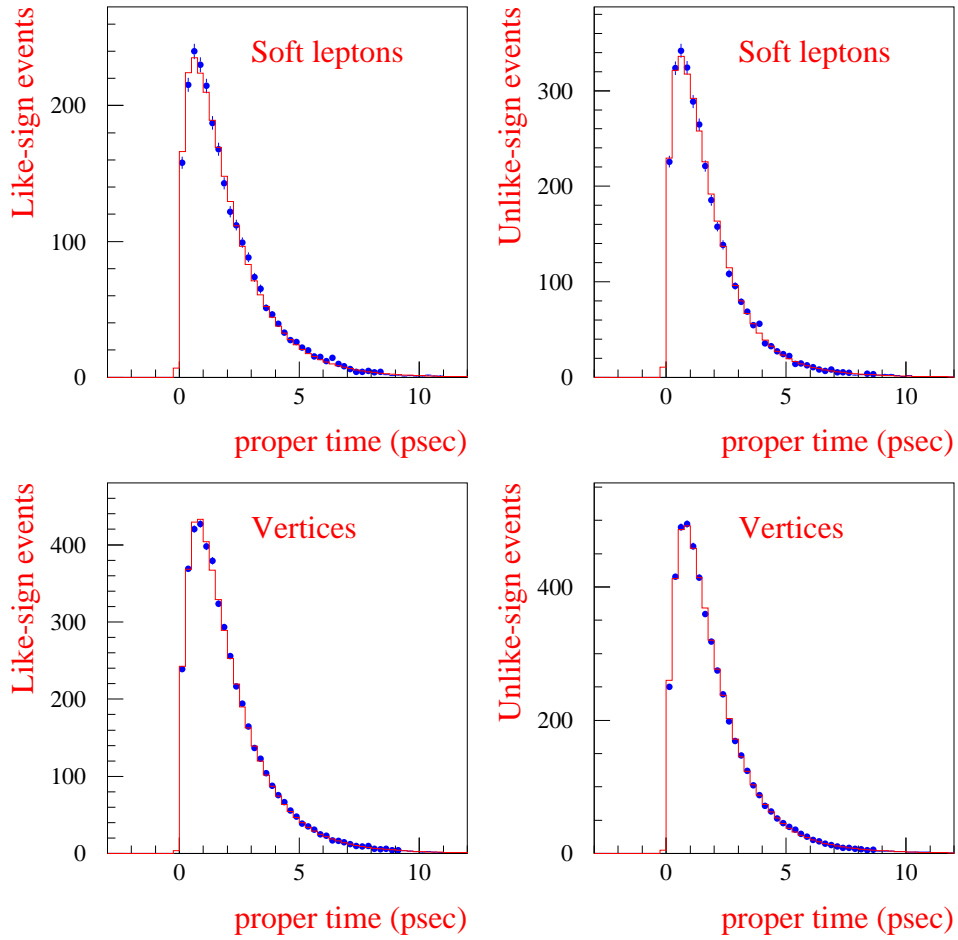


Figure 8: Like- and unlike-sign events as a function of the proper time for the soft leptons and inclusive vertices. The 1994 and 1995 data are shown in dots, the fitted parametrization is shown as a solid line.

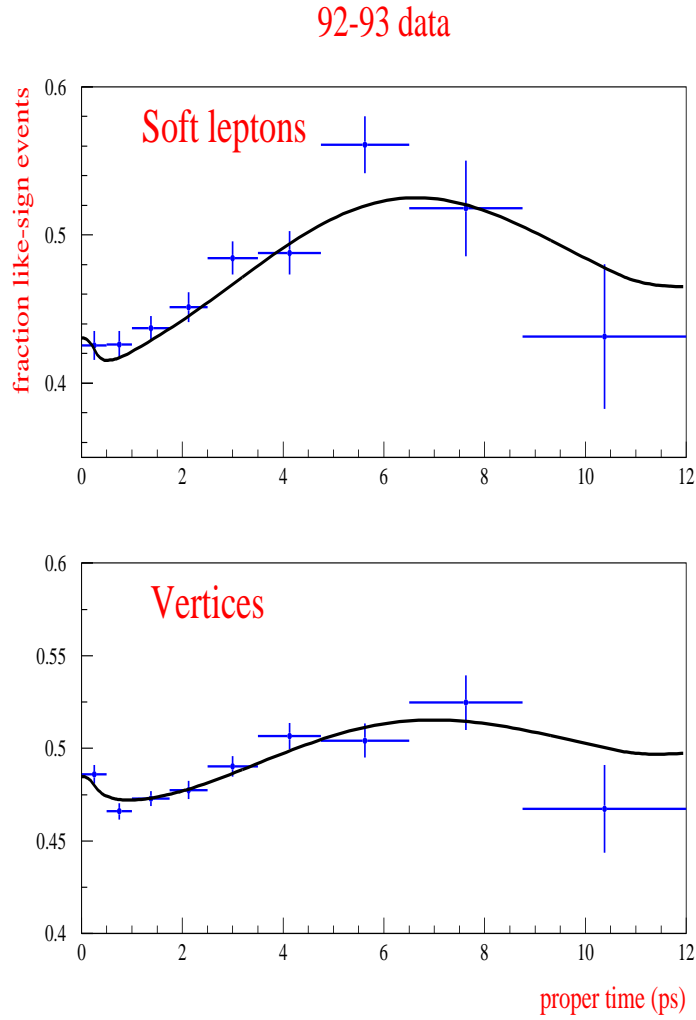


Figure 9: Fraction of like-sign events as a function of the proper time for the soft leptons and inclusive vertices. The 1992 and 1993 data are shown in dots, the parametrization is shown as a solid line.

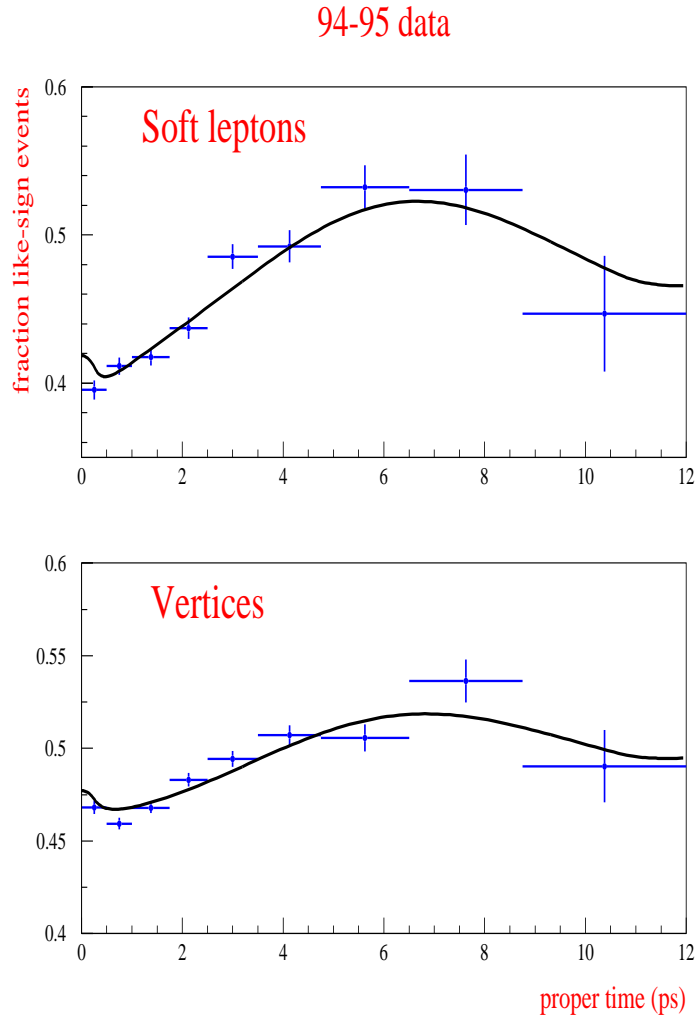


Figure 10: Fraction of like-sign events as a function of the proper time for the soft leptons and inclusive vertices. The 1994 and 1995 data are shown in dots, the parametrization is shown as a solid line.

## 2.7 Measurement of the $B_d$ oscillations

The mass difference between the two  $B_d$  states was determined by fitting the fraction of like-sign events as a function of the reconstructed proper time. The following function was used:

$$\begin{aligned}
N_{like} &= A(t) f_{Bu} \frac{e^{-t/\tau_{Bu}}}{\tau_{Bu}} (1 - \epsilon_b) \\
&+ A(t) f_{Bbaryon} \frac{e^{-t/\tau_{Bbaryon}}}{\tau_{Bbaryon}} (1 - \epsilon_b) \\
&+ A(t) f_{Bs} \frac{e^{-t/\tau_{Bs}}}{2\tau_{Bs}} \\
&+ A(t) f_{Bd} \frac{e^{-t/\tau_{Bd}}}{2\tau_{Bd}} [(1 - 2\epsilon_d) \cos(\Delta m_d t) + 1] \\
&+ (1 - \epsilon_c) f_c N_c(t) + (1 - \epsilon_{uds}) f_{uds} N_{uds}(t)
\end{aligned} \tag{20}$$

$$N_{tot} = \sum A(t) f_{Bi} e^{-t/\tau_{Bi}} / \tau_{Bi} + f_c N_c(t) + f_{uds} N_{uds}(t) \tag{21}$$

The values for  $f_{Bi}$  and the B lifetimes were fixed at the values listed in Table 2.4. The background fraction  $f_c$ ,  $f_{uds}$  and the functions  $N_c(t)$  and  $N_{uds}$  as well as the acceptance  $A(t)$  were parametrized using the simulation. The tagging purities  $\epsilon_c$  and  $\epsilon_{uds}$  were taken from the simulation.

The fit had four free parameters:  $\epsilon_d$  the  $B_d$  tagging purity,  $\Delta m_d$  the  $B_d$  mass difference,  $\epsilon_b$  is parametrized as:  $\epsilon_b = R1 e^{at} + R2 e^{-t}$ , where R1 and R2 are left free in the fit. The parameter  $R2$  takes into account the slight dependence of the tagging purity as a function of the proper time. The parameter  $a$  was fitted on the simulated data and then fixed to its value of  $4.8 \cdot 10^{-3}$ . The reason for performing a four parameter fit is that both tagging purity of the  $B_d$  and the other B particles are determined on the data. Therefore systematic uncertainties on these parameters were largely reduced. In this way the fit results becomes also less sensitive to e.g. the fraction of  $B_s$  particles.

The fit was performed in the range from 0.5 to 12 ps. The results for the different parameters are:  $\epsilon_d = 0.583 \pm 0.011$  (0.5803) and  $R1 = 0.536 \pm 0.0062$  (0.5448),  $R2 = 0.0944 \pm 0.029$  (0.0632). In brackets the result of a fit to the simulation is shown.

The fit result for the  $B_d$  mass difference is  $\Delta m_d = 0.508 \pm 0.027$  (stat.) with a  $\chi^2/ndof = 23.36/(23-4)$ .

A breakdown of the systematical errors affecting the measurement is shown in Table 6. The fractions of  $B_s$  and B baryons in the sample were changed (correspondingly the other B fractions are recalculated) as well as the lifetimes and backgrounds. The resolution function is smeared by an additional gaussian term with a width of  $0.1+0.03t$  ps. Note that changing the resolution by a relative 10% gave only a shift on  $\Delta m_d$  of  $0.0018 \text{ ps}^{-1}$ . The total systematic error amounts to  $0.007 \text{ ps}^{-1}$ .

The final result is thus:

$$\Delta m_d = 0.508 \pm 0.027 \text{ (stat)} \pm 0.007 \text{ (syst.)}.$$

The total error is therefore 0.028.

The result for the mass difference of the two physical  $B_d^0$  states is compatible with the results from other experiments [8].

A fit is done to extract the width difference  $\Delta\Gamma_{Bd}$ . In the fit the expression in Eq.(20)  $[(1 - 2\epsilon_d) \cos(\Delta m_d t) + 1]$  is replaced by  $[(1 - 2\epsilon_d) \cos(\Delta m_d t) + \cosh(\Delta\Gamma_{Bd} t/2)]$  and the expression in Eq.(21) is modified. The result of the five parameter fit is  $\Delta\Gamma_{Bd} = 0. \pm$

Inclusive vertices and soft leptons

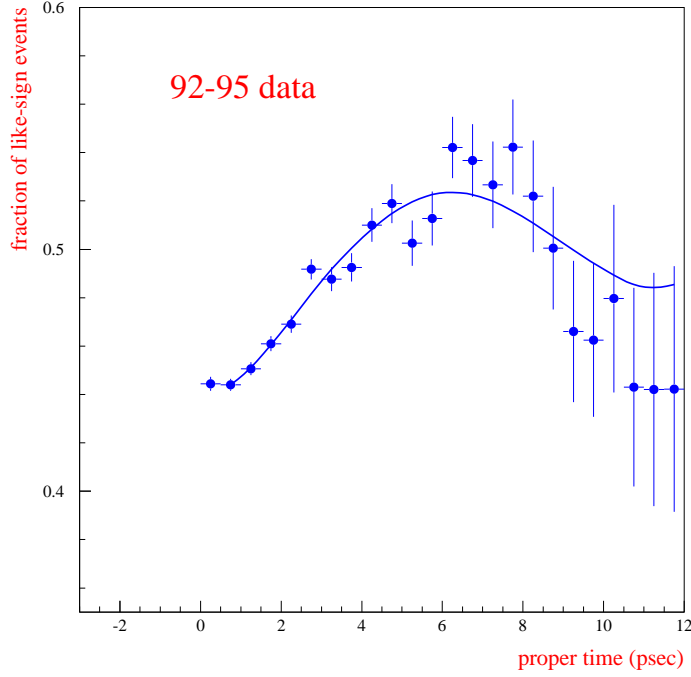


Figure 11: Fraction of like-sign events as a function of the proper time using 1992-1995 data. The data is shown with error bars, the solid line corresponds to the fit.

$0.079 \text{ ps}^{-1}$ . The total systematic error was evaluated for the error sources listed in Table 6 and found to be  $0.0002 \text{ ps}^{-1}$ . Using the measured  $B_d$  lifetime  $\tau_{B_d} = 1.55 \pm 0.05 \text{ ps}$  [8],  $\Delta\Gamma_{B_d}/\Gamma_{B_d} = 0. \pm 0.12$  (*total*). The following upper limit was derived:

$$\Delta\Gamma_{B_d}/\Gamma_{B_d} < 0.20 \text{ at } 90\% \text{ CL.}$$

error source	values	systematic error on $\Delta m_d$ ( $\text{ps}^{-1}$ )
$f_{B_s}$	0.097 to 0.108	-0.00021
$f_{B \text{ baryon}}$	0.103 to 0.12	0.00039
$\tau_{B_s}$	1.55 to 1.65 ps	0.0002
$\tau_{B^+}$	1.65 to 1.67 ps	-0.0008
$\tau_{B_d}$	1.55 to 1.58 ps	0.0012
$\tau_{B \text{ baryon}}$	1.2 to 1.25 ps	-0.0008
uds background scale factor	1 to 1.10	-0.00022
charm background scale factor	1 to 1.10	0.00052
tagging factor C	1 to 0.95 (0.85)	0.0006
scale factor proper time	1 to 1.01	-0.0049
resolution smearing		0.0037
Total systematic error		0.0067

Table 6: The systematic errors affecting the  $\Delta m_d$  measurement.

## 2.8 Search for $B_s$ oscillations

To search for the  $B_s$  oscillations a likelihood fit was performed, where the likelihood is defined as:

$$\mathcal{L} = - \sum_{\text{like-sign}} \ln(\mathcal{P}^{\text{like}}(t_{\text{rec}}, P_{\text{comb}}, P_{\text{decay}})) - \sum_{\text{unlike-sign}} \ln(\mathcal{P}^{\text{unlike}}(t_{\text{rec}}, P_{\text{prod}}, P_{\text{decay}})) \quad (22)$$

To extract results from this fit the so-called amplitude method was used [9]. For the mixed and unmixed  $B_s$  probability the following expressions were used:

$$\mathcal{P}_{B_s^0}^{\text{unmix.}} = \frac{1}{2\tau_{B_s}} e^{-\frac{t}{\tau_{B_s}}} [1 + A \cos(\Delta m_s t)] \quad (23)$$

and similarly:

$$\mathcal{P}_{B_s^0}^{\text{mix.}} = \frac{1}{2\tau_{B_s}} e^{-\frac{t}{\tau_{B_s}}} [1 - A \cos(\Delta m_s t)] \quad (24)$$

The oscillation amplitude  $A$  and its error  $\sigma_A$  were fitted on the data as a function of  $\Delta m_s$ . The result of the amplitude fit is shown in Figures 12 and 13.

Before discussing the result and its interpretation, the systematic errors have been studied. This was done by changing one parameter e.g.  $f_{B_s}$  and redoing the full amplitude fit. The systematic error was then evaluated as [9]:

$$\sigma_A^{\text{sys}} = A_1 - A_0 + (1 - A_0) \frac{\sigma_{A_1}^{\text{stat}} - \sigma_{A_0}^{\text{stat}}}{\sigma_{A_1}^{\text{stat}}}, \quad (25)$$

where  $A_0(A_1)$  and  $\sigma_{A_0}(\sigma_{A_1})$  denote the fitted amplitude and error before (after) changing the parameter. The following parameters have been changed:

- $f_{B_s}$  from 0.097 to 0.108,
- the uds and charm backgrounds have been scaled up by 10%,
- the tagging purity has been changed by 5% for the soft, leptons and by 15% for the inclusive vertices by changing the correction factor  $C$ ,
- the width of the resolution function for the constant term  $\sigma_0$  has been changed by 10%,
- the width of the resolution function for the momentum term  $\sigma_p$  has been changed by 10%.

The total systematic error as a function of  $\Delta m_s$  is shown in Figure 12b. The systematic error is at most 20% of the statistical error.

Using the results for the amplitude and its error it is possible to obtain the 95% CL exclusion region. This region corresponds to  $A + 1.645\sigma_A$ . This curve is shown in Figures 12 and 13. From the data one can conclude that no  $B_s^0$ - $\bar{B}_s^0$  oscillations have been observed. A limit on the mass difference of the two physical  $B_s^0$  states can be put:

$$\Delta m_s > 1.1 ps^{-1} \text{ at } 95 \% \text{ CL.}$$

Using the error on  $A$ ,  $\sigma_A$  one can extract the sensitivity or the expected limit on  $\Delta m_s$  at 95% CL:

$$\text{Sensitivity} = 6.1 ps^{-1}.$$

The sensitivity would be  $6.2 ps^{-1}$  if the systematic error on the amplitude was neglected. Note that the range from  $\Delta m_s = 1.5$  to  $5.3 ps^{-1}$  is also excluded by the data at 95 % CL.

## Inclusive vertices and soft leptons

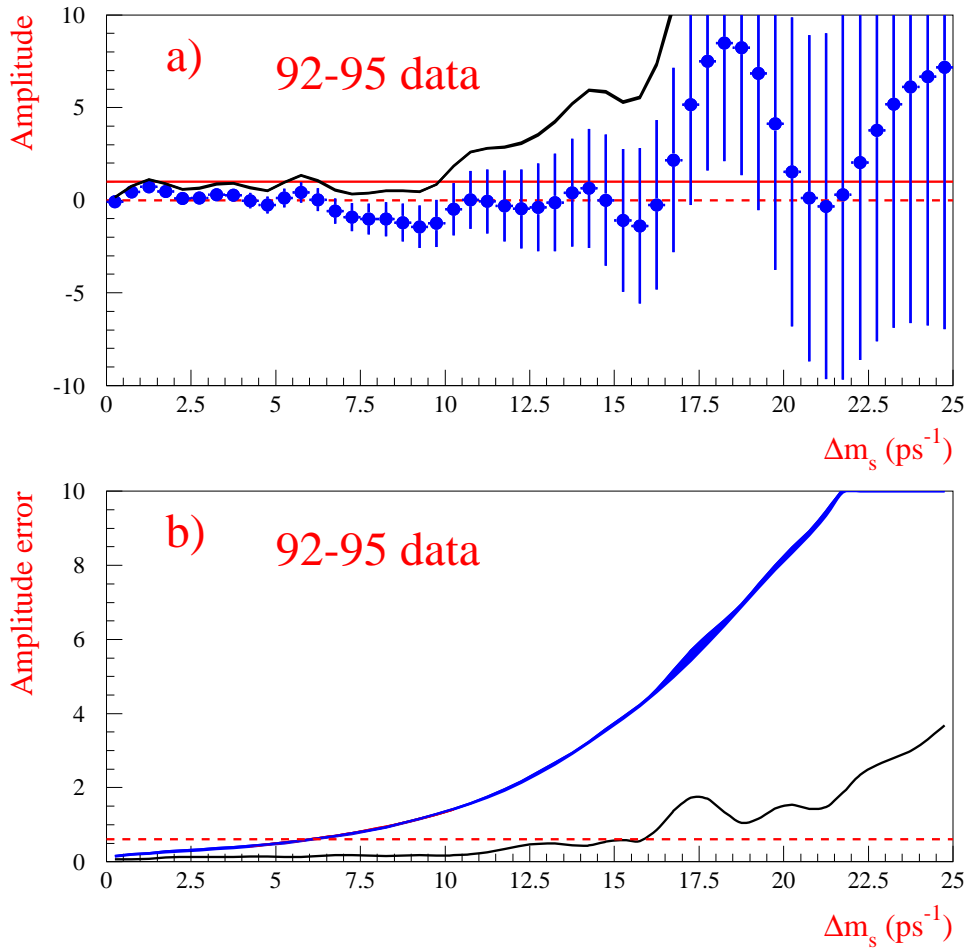


Figure 12: Figure a) Fitted amplitude as a function of  $\Delta m_s$ . The horizontal line corresponds to amplitude  $A=1$ . The black area corresponds to the curves for  $A + 1.645\sigma_{A_{stat}}$  and  $A + 1.645\sigma_{A_{tot}}$ . Figure b) shows the total amplitude error as a function of  $\Delta m_s$ . The blue area corresponds to statistical error  $\sigma_{A_{stat}}$  and total error  $\sigma_{A_{tot}}$ . The lower curve shows the systematical error  $\sigma_{A_{sys}}$ . The horizontal dashed line corresponds to the expected 95% CL limit.



## Inclusive vertices and soft leptons

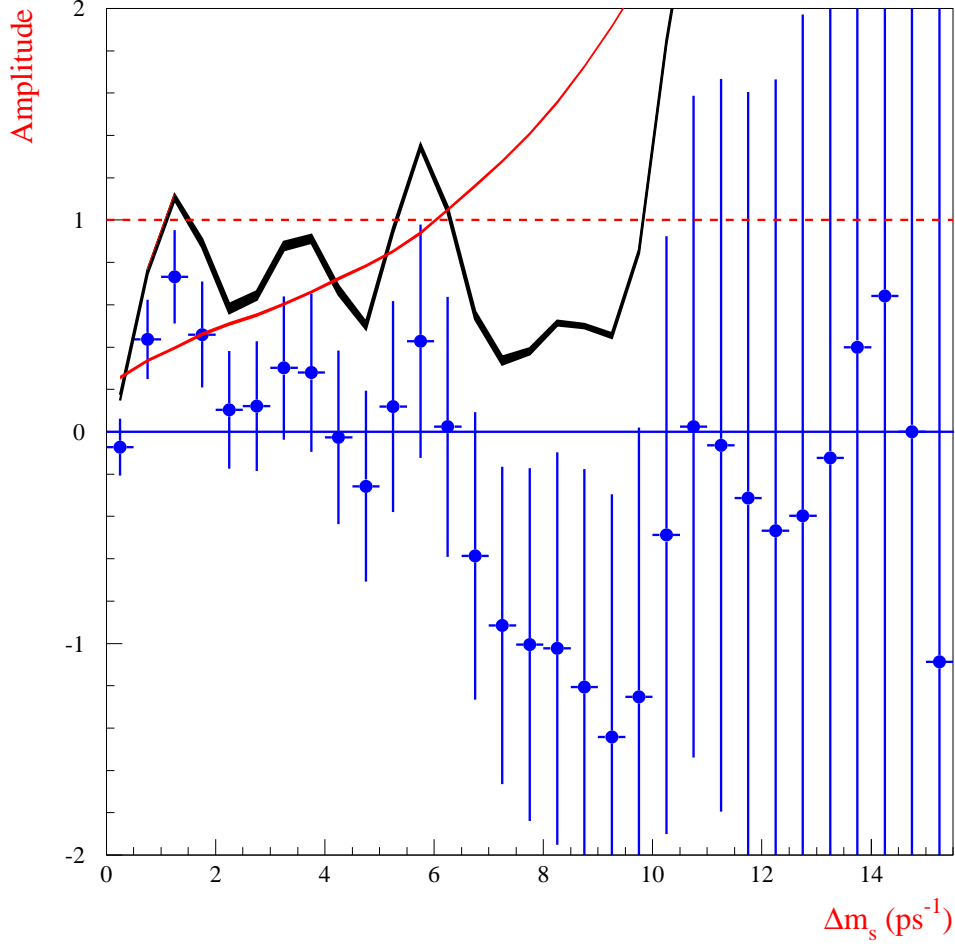


Figure 13: Fitted amplitude as a function of  $\Delta m_s$ . The dashed horizontal line corresponds to amplitude  $A=1$ . The black area corresponds to the curves for  $A + 1.645\sigma_{A_{stat}}$  and  $A + 1.645\sigma_{A_{tot}}$ . The rising red curve corresponds to  $1.645\sigma_{A_{tot}}$ . The crossing point with  $A=1$  at  $\Delta m_s = 6.1 \text{ ps}^{-1}$  gives the expected upper limit at 95% CL.

### 3 Conclusion

Using samples of soft leptons and inclusive vertices the mass difference of the two physical  $B_d^0$  states was measured to be:

$$\Delta m_d = 0.508 \pm 0.027(stat.) \pm 0.007(syst.)ps^{-1}$$

The following limit on the width difference of the two physical  $B_d^0$  was obtained:

$$\Delta\Gamma_{Bd}/\Gamma_{Bd} < 0.20 \text{ at } 90\% \text{ CL.}$$

No evidence for  $B_s^0 - \overline{B}_s^0$  oscillations was found and a limit on the mass difference of the two physical  $B_s^0$  states was put:

$$\Delta m_s > 1.1ps^{-1} \text{ at } 95\% \text{ CL}$$

with a

$$\text{Sensitivity} = 6.1 ps^{-1}.$$

## References

- [1] F. Parodi, P. Roudeau and A. Stocchi, *Il Nuovo Cimento* Vol. 112 A,N.8 (Agosto 1999)  
M. Ciuchini, F. Franco, L.Giusti, V.Lubicz, G. Martinelli, hep-ph/9910236  
F. Caravaglios, F. Parodi, P. Roudeau, A. Stocchi, hep-ph/00 02171
- [2] DELPHI Coll., P. Abreu et al., *Eur. Phys. J. C*13 (2000) 57,  
DELPHI Coll., P. Abreu et al., *Eur.Phys.J C*18 (2000) 229,  
DELPHI Coll., P. Abreu et al., *Eur. Phys. J. C*16 (2000) 555.
- [3] DELPHI Collaboration, Search for  $B_s - \overline{B}_s^0$  oscillations, contribution to ICHEP 2000 # 380 and DELPHI 200-104 CONF 403.
- [4] DELPHI Collaboration, P. Aarnio et al., *Nucl. Inst. Meth.* **A303**(1991)233, DELPHI Collaboration, P. Abreu et al., *Nucl. Inst. Meth.* **A378**(1996)57.
- [5] G.V. Borisov and C. Mariotti, *Nucl. Instr. and Meth.* **A372** (1996) 181 G. V. Borisov *Combined b-tagging*, DELPHI Note, PHYS 716, 94, 1997
- [6] T. Sjostrand, *PYTHIA 5.7 and JETSET 7.4*, *Computer Physics Commun.* 74. 1994
- [7] DELPHI Collaboration, “DELSIM Reference Manual”, DELPHI 87-97 PROG-100.
- [8] ALEPH, CDF, DELPHI, L3, OPAL, SLD Collaboration, “ Combined results on b-hadron production rates, lifetimes, oscillations and semileptonic decays “, CERN-EP-2000-096.  
The most recent update [http://lepbos.web.cern.ch/LEPBOSC/combined\\_results/Moriond\\_QCD\\_2001/](http://lepbos.web.cern.ch/LEPBOSC/combined_results/Moriond_QCD_2001/).
- [9] H.G. Moser and A. Roussarie, *Nucl. Instr. and Meth.* **A384** (1997) 491.